

Zeno crossovers in the entanglement speed of spin chains with noisy impurities

Abhijit P Chaudhari,^{1,2} Shane P Kelly,² Riccardo Javier Valencia Tortora,² and Jamir Marino²

¹*Department of Physics, Indian Institute of Technology (Banaras Hindu University), Varanasi - 221005, India*^{*}

²*Institut für Physik, Johannes Gutenberg Universität Mainz, D-55099 Mainz, Germany*

(Dated: June 1, 2022)

We study a one dimensional quantum XY spin chain driven by a local noisy spin impurity with finite correlation time, along the transverse field direction. We recover the celebrated Zeno crossover and we show that entanglement can be used as a proxy for the heating and strong-measurement regimes. We compute the entanglement entropy of a block of spins and we observe that its velocity spreading decreases at strong dissipation, as a result of the Zeno effect. Upon increasing the correlation time of the noise, the location of the Zeno crossover shifts at stronger dissipation rates opening up a broader heating phase. We offer insight on the mechanisms underlying the dynamics of the entanglement entropy by monitoring different time traces of the local transverse magnetisation profile. Our results aim at starting a complementary viewpoint on the field of dissipative quantum impurities, based on a theoretical quantum information perspective.

I. INTRODUCTION

Impurity models represent a traditional avenue [1, 2] for developing intuition in complex many-body problems ranging from condensed matter physics to solid state and encompassing cold atoms. A recent line of investigation is extensively revisiting instances of prototypical impurity systems in a dissipative setting, with the aim to provide future guidance in the solution of the driven-dissipative quantum many-body problem. The effect of a localised dissipative potential can be implemented, for instance, by shining an electron beam on an atomic BEC [3, 4], and it results in a decrease of atom losses at strong dissipation rate. This is a manifestation of a many-body version of the Zeno effect [5–10], where the usual slowdown of transport at strong measurement is at interplay with many-particle correlation effects [11]. Furthermore, losses provided by a near-resonant optical tweezer at a quantum point contact, can realise a dissipative scanning gate microscope for ultra-cold ⁶Li atoms [12, 13], offering a resource for transport problems. At the same time, like in their unitary counterparts, dissipative impurities can also have an intrusive effect and significantly rearrange the properties of many-body states as in the Anderson impurity problem [2, 14]. A classification of the phenomenology of dissipative impurities is currently subject of vivid research at the interface of quantum information, atomic physics, quantum optics and solid state [15–22]; it comprises driven-dissipative boundary spin problems [23–29], and the realisation of the many-particle Zeno effect in lossy (and noisy) condensed matter systems and cold atoms [30–34].

The onset of the Zeno effect is marked by strong suppression of dynamical observables (such as decay rates or currents) beyond a certain dissipation strength. In this work, we take one step further and we inspect whether entanglement quantifiers can expose the Zeno crossover

which separates the heating phase from the transport-impeded regime. Specifically, we consider an exactly solvable instance of the problem, extending previous results on locally noise-driven free fermions [35], in order to evaluate the entanglement entropy of a block of spins. The Gaussian nature of the problem allows to average over several stochastic realisations, and to follow dynamics for long times and large system sizes, and we show that the growth rate of the entanglement entropy carries a hallmark of the Zeno transition. Our results have the potential to bridge the growing field of dissipative impurities in condensed matter systems with theoretical quantum information science, and stimulate a new line of investigation at their interface.

II. MODEL

We study the quantum XY spin chain [36]

$$H_0 = - \sum_{i=-L}^L (1 + \gamma) \sigma_i^x \sigma_{i+1}^x + (1 - \gamma) \sigma_i^y \sigma_{i+1}^y + h \sigma_i^z, \quad (1)$$

where σ_i^α , ($\alpha = x, y, z$) are the Pauli matrices for the i^{th} spin along the direction α , and $0 \leq \gamma \leq 1$. The system is considered to be periodic ($\sigma_i^{x,y,z} = \sigma_{N+i}^{x,y,z}$). However the results for the dynamics obtained here are equally valid for free boundaries as they apply to the bulk of the system. At $t = 0$, the system is prepared in the ground state of H_0 and at subsequent times, we suddenly turn on a time varying stochastic field which drives the spin impurity at the site $i = 0$:

$$H(t) = H_0 + \sqrt{\kappa} \eta(t) \sigma_0^z. \quad (2)$$

The time varying stochastic field $\eta(t)$ is an Ornstein-Uhlenbeck (OU) process [37] with $\langle \eta(t_1) \eta(t_2) \rangle = \exp\left(-\frac{|t_1 - t_2|}{\tau}\right)/\tau$. When $\tau \rightarrow 0$, $\eta(t)$ is equivalent to Gaussian white noise and we will work in this limit for

* apravin.chaudhari.phy16@iitbhu.ac.in

the rest of the paper unless otherwise stated (cf. with Sec. V A). In this regime, the following Linbladian evolution is equivalent to the stochastic Schrodinger equation (SSE) with Hamiltonian in Eq. 2,

$$\partial_t \hat{\rho}(t) = -i[\hat{H}_0, \hat{\rho}(t)] + \frac{\kappa}{2}[\sigma_0^z, [\hat{\rho}(t), \sigma_0^z]]. \quad (3)$$

To compute the time evolution of any observable O , we average over noise realisations

$$O(t) = \langle O_\eta(t) \rangle_\eta, \quad \text{with} \quad O_\eta(t) = O[\hat{\rho}_\eta(t)], \quad (4)$$

where $\hat{\rho}_\eta(t)$ is the density matrix for a given noise realisation $\eta(t)$ and $O[\hat{\rho}_\eta(t)]$ is a functional of $\hat{\rho}_\eta(t)$. The approaches in Eq. (3) and (4) are connected via the identity $\hat{\rho} = \langle \hat{\rho}_\eta(t) \rangle_\eta$.

Using the Jordan-Wigner transformation [36] we map $\hat{H}(t)$ to a system of free fermions and consider the even sector ($c_i = -c_{N+i}$):

$$\begin{aligned} \hat{H}(t) = \sum_{i=-L}^L & - (c_i^\dagger c_{i+1} + c_{i+1}^\dagger c_i) - \gamma (c_i^\dagger c_{i+1}^\dagger + c_{i+1} c_i) - h (c_i c_i^\dagger - c_i^\dagger c_i) \\ & + \sqrt{\kappa} \eta(t) (c_0 c_0^\dagger - c_0^\dagger c_0). \end{aligned} \quad (5)$$

In vectorial notation

$$\mathbf{c} = \begin{pmatrix} c_{-L} \\ \vdots \\ c_L \end{pmatrix}, \quad \bar{\mathbf{c}} = \begin{pmatrix} \mathbf{c} \\ \mathbf{c}^\dagger \end{pmatrix}, \quad (6)$$

$\hat{H}(t)$ can be expressed as

$$\hat{H}(t) = \bar{\mathbf{c}}^\dagger (M + \sqrt{\kappa} \eta(t) \mathbf{L}) \bar{\mathbf{c}} \quad (7)$$

where

$$M = \begin{bmatrix} \alpha & -\beta \\ \beta & -\alpha \end{bmatrix}, \quad \mathbf{L} = \begin{bmatrix} -\mathbf{L} & 0 \\ 0 & \mathbf{L} \end{bmatrix}. \quad (8)$$

M is the single particle Hamiltonian associated with the coherent part, H_0 , from $H(t)$ and \mathbf{L} represents the noise term σ_0^z from $H(t)$. The matrix elements read

$$\begin{aligned} \alpha_{i,j} &= -(\delta_{i,j+1} + \delta_{i,j-1} - \delta_{i,-\frac{(N-1)}{2}} \delta_{j,\frac{(N-1)}{2}} - \delta_{i,\frac{(N-1)}{2}} \delta_{j,-\frac{(N-1)}{2}}) + h \delta_{i,j}, \\ \beta_{i,j} &= \gamma (\delta_{i,j+1} - \delta_{i,j-1} + \delta_{i,-\frac{(N-1)}{2}} \delta_{j,\frac{(N-1)}{2}} - \delta_{i,\frac{(N-1)}{2}} \delta_{j,-\frac{(N-1)}{2}}), \\ \mathbf{L}_{i,j} &= \delta_{i,0} \delta_{j,0}, \end{aligned} \quad (9)$$

where ($i, j = -L, \dots, L$) are the real space indices of the chain. The matrix α contains hopping amplitudes between any two lattice sites on the chain while β encodes superconducting terms between any two lattice sites on the chain. Since $H(t)$ is Hermitian, this implies $\alpha^T = \alpha$ and $\beta^T = -\beta$.

When $\gamma = 0$, the local impurity, $\eta(t) \sigma_0^z$, corresponds to a noise field coupled to the density of Jordan-Wigner fermions [35]. However, when $\gamma \neq 0$ [36], a Bogolyubov rotation is necessary to bring (5) in diagonal form; the representation of σ_0^z will therefore contain several other non trivial terms in addition to fermion density. In order to appreciate that, we write σ_0^z in terms of the Jordan-

Wigner fermions

$$\sigma_0^z = 1 - 2\hat{n}_0 = 1 - 2c_0^\dagger c_0 = 1 - \frac{2}{2L+1} \sum_{p,q} c_{-p}^\dagger c_q, \quad (10)$$

where in the last equality we moved to Fourier space. We now rewrite this expression by employing a Bogolyubov rotation [36]

$$c_q = u_q \alpha_q + i v_q \alpha_{-q}^\dagger \quad (11)$$

$$(12)$$

$$c_{-q}^\dagger = u_q \alpha_{-q}^\dagger + i v_q \alpha_q, \quad (13)$$

where $u_q = \cos(\theta_q/2)$ and $v_q = \sin(\theta_q/2)$, and θ_q is the

$O(2)$ rotation angle for a given mode q

$$\tan \theta_q = \frac{\gamma \sin q}{h - \cos q}. \quad (14)$$

Therefore, Eq. 10 becomes

$$\sigma_0^z = 1 - \frac{2}{2L+1} \sum_{p,q} i u_q v_p \alpha_p \alpha_q + i u_p v_q \alpha_{-p}^\dagger \alpha_{-q}^\dagger - v_p v_q \alpha_p \alpha_{-q}^\dagger + u_q u_p \alpha_{-p}^\dagger \alpha_q \quad (15)$$

Eq. (15) shows that σ_0^z does not simply act as a local dephasing but also contains two body losses and pumps processes ($\alpha_p \alpha_q$ and $\alpha_{-p}^\dagger \alpha_{-q}^\dagger$, respectively) for any non-zero γ . This sets our work apart from the pre-existing literature where localised losses, gains or only dephasing are considered individually.

III. PRE-RELAXATION DYNAMICS

The dynamics start from the ground state of the XY chain without the impurity which is Gaussian. The Gaussian nature of the state is preserved during evolution for

each noise realisation; this fact will be crucial for the evaluation of the entanglement entropy (cf. Sec. IV).

We first evaluate the dynamics of the local magnetisation, $m(x, t) = \langle \sigma_x^z(t) \rangle$, as a function of its position along the chain, x , and at time, t . In order to investigate this quantity, we turn to the adjoint master equation which takes the following form, given that the jump operator is Hermitian,

$$\partial_t \langle A \rangle = \partial_t (\text{Tr}(\hat{A} \hat{\rho}(t))) = i \langle [H_0, \hat{A}] \rangle + \frac{\kappa}{2} \langle [\sigma_0^z, [\hat{A}, \sigma_0^z]] \rangle. \quad (16)$$

We use (16) to obtain the equations of motions for the two point correlators, $C_{i,j} = \langle c_i^\dagger(t) c_j(t) \rangle$ and $F_{i,j} = \langle c_i^\dagger(t) c_j^\dagger(t) \rangle$:

$$\partial_t \mathcal{C} = -i[M, \mathcal{C}] - 2\kappa \begin{bmatrix} -\mathbf{L}\mathbf{C} - \mathbf{C}\mathbf{L} + 2\mathbf{L}\mathbf{C}\mathbf{L} & \mathbf{L}\mathbf{F}^\dagger + \mathbf{F}^\dagger\mathbf{L} + 2\mathbf{L}\mathbf{F}^\dagger\mathbf{L} \\ \mathbf{L}\mathbf{F}^\dagger + \mathbf{F}^\dagger\mathbf{L} + 2\mathbf{L}\mathbf{F}^\dagger\mathbf{L} & \mathbf{L}\mathbf{C} + \mathbf{C}\mathbf{L} - 2\mathbf{L}\mathbf{C}\mathbf{L} \end{bmatrix} \quad (17)$$

where

$$\mathcal{C} = \begin{bmatrix} 1 - C & F^\dagger \\ F & C \end{bmatrix}. \quad (18)$$

Finally, $m(x, t) = 1 - 2C_{x,x}(t)$. The stochastic impurity locally perturbs the chain which results in emission of pairs of Bogolyubov quasi-particles. They move with a velocity $v_p = \partial_p \epsilon(p)$, where $\epsilon(p) = 4((\cos(p) + h)^2 + (\gamma \sin(p))^2)^{\frac{1}{2}}$ (see for instance [36]). This gives rise to a ballistic density front which can be seen in Fig. 1.

When $\gamma = 0$, the system is invariant under rotations along the \hat{z} -axis and the global magnetisation along \hat{z} is conserved. We see an emergence of oscillations in the vicinity of the impurity followed by a ballistic density front. The conservation of the total magnetisation along \hat{z} breaks for $\gamma \neq 0$, which results in amplification of the oscillations and expansion of the spatial extent of the ballistic density front as compared to the $\gamma = 0$ case, at any given time. We also observe that the overall speed of the ballistic density front reduces as γ increases (see Fig. 1). The overall slowing down of the ballistic density front is expected from the group velocity, as $v_p^{\max} \propto 1/\gamma$

(cf. with the expression for $\epsilon(p)$). As γ increases, at any given time the expansion of ballistic front and its slowing taken together reduces the spatial extent over which the oscillations emerge. This explains the absence of oscillations for $\gamma = 1$ and the weak oscillations for $\gamma = 0.5$, in Fig. 1.

Dynamics do not 'realize' immediately the breaking of rotational invariance along \hat{z} : this is evident from the time evolution of $M(\gamma, t)$ with respect to $M(\gamma, 0)$ (cf. inset in Fig. 1). For all the values of γ , $M(\gamma, t)$ does not increase appreciably as compared to its initial value $M(\gamma, 0)$ up to time scales of the order of $1/\gamma$, in a fashion reminiscent of 'pre-relaxation' effects in integrable systems [38, 39].

IV. ENTANGLEMENT ENTROPY AS A PROBE OF THE ZENO CROSSOVER

A. Numerical Scheme

As mentioned in the previous section, the stochastic drive emits entangled pairs of quasi-particles which

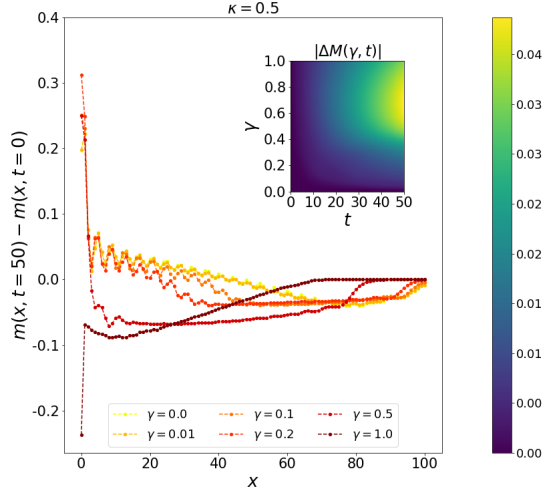


FIG. 1: Local magnetisation as a function of x and t , for $L = 100$ and $h = \sqrt{2}$. The initial local magnetisation profile ($m(x, t = 0)$), strongly depends on γ . Hence, to study the effect of γ on the dynamics ensued by the impurity, we subtract it from local magnetisation profile. Notice that irrespective of the value of γ , we see a ballistic density front emitted by the impurity. For small γ (such as $\gamma = 0.01$), the local magnetisation profile does not differ appreciably from the profile obtained for $\gamma = 0$. This similarity fades away as γ increases and reaches its maximum value. The inset shows a density plot of absolute value of the global magnetisation with reference to its initial value ($\Delta M(\gamma, t) = M(\gamma, t) - M(\gamma, 0)$). The magnitude of $\Delta M(\gamma, t)$ increases from lighter to darker region. The system appreciably realises the effect of the breaking of rotational invariance along \hat{z} , after a time scale $t \sim 1/\gamma$.

leads to generation of entanglement, similarly to local quenches in closed systems. Hence, we turn our attention to the resultant entanglement dynamics. We use the Von-Neumann entropy (EE) of the reduced density matrix to quantify entanglement for the block $[x_1, x_2]$

$$S_{ent}^\eta(t) = -\text{Tr}[\rho_{[x_1, x_2]}^\eta \log_2 \rho_{[x_1, x_2]}^\eta], \quad (19)$$

where $\rho_{[x_1, x_2]}^\eta = \text{Tr}_{[x_1, x_2]^c} [|\psi(t)\rangle\langle\psi(t)|]$ and $\text{Tr}_{[x_1, x_2]^c}$ refers to partial trace over the remainder of the chain. For the rest of the paper, we will be interested in $\langle S_{ent}^\eta(t) \rangle_\eta$ of the conditional state $\hat{\rho}_\eta(t) = |\psi(t)\rangle\langle\psi(t)|$, averaged over all noise realisations. We choose to study this quantity over the S_{ent} of the mean state $\hat{\rho}(t) = \langle \hat{\rho}_\eta(t) \rangle_\eta$ since in the long time limit the latter turns into an infinite temperature state, and the entanglement entropy would be trivial.

The SSE associated to Eq. (2) preserves the Gaussianity of the initial state and hence at any time, the state of the system is fully characterised by the two point correlation functions

$$C_{i,j}^\eta(t) = \langle c_i^\dagger(t) c_j(t) \rangle, F_{i,j}^\eta(t) = \langle c_i^\dagger(t) c_j^\dagger(t) \rangle. \quad (20)$$

The task of calculating $S_{ent}^\eta(t)$ for a given realisation reduces to obtaining the correlation matrix $\hat{\phi}^\eta(t)$ at any given time. We Trotterize the time evolution and we use as initial condition the correlations of the ground state

$\hat{\phi}(0)$. The entanglement entropy equals to [40]

$$S_{ent}^\eta(t) = -\sum_{p=1}^{2q} [\lambda_p \log_2 \lambda_p]. \quad (21)$$

where $\{\lambda_p\}$ are the eigenvalues of the matrix

$$\hat{\phi}_{sub}^\eta(t) = \begin{bmatrix} (1 - C^\eta(t))_{i,j=x_1}^{x_2} & ((F^\eta(t))^\dagger)_{i,j=x_1}^{x_2} \\ (F^\eta(t))_{i,j=x_1}^{x_2} & (C^\eta(t))_{i,j=x_1}^{x_2} \end{bmatrix}. \quad (22)$$

Finally, we average $S_{ent}^\eta(t)$ obtained for a single realisation of the stochastic field, over a large number of realisations ($N_\eta \sim 10^4$). In the following, we focus on a block of spins in the interval $[x_1, x_2]$ with $x_1 = 0$ and $x_2 = L$.

We also investigate the following fluctuation correlation function formerly introduced in [35]

$$\Delta_{LR}^\eta = \langle \hat{N}_R \hat{N}_L \rangle - \langle \hat{N}_L \rangle \langle \hat{N}_R \rangle, \quad (23)$$

where \hat{N}_L represents the total number of fermions on l sites to the left of the impurity (we fix $l = 5$)

$$\hat{N}_L \equiv \sum_{i=-l}^{-1} \hat{n}_i. \quad (24)$$

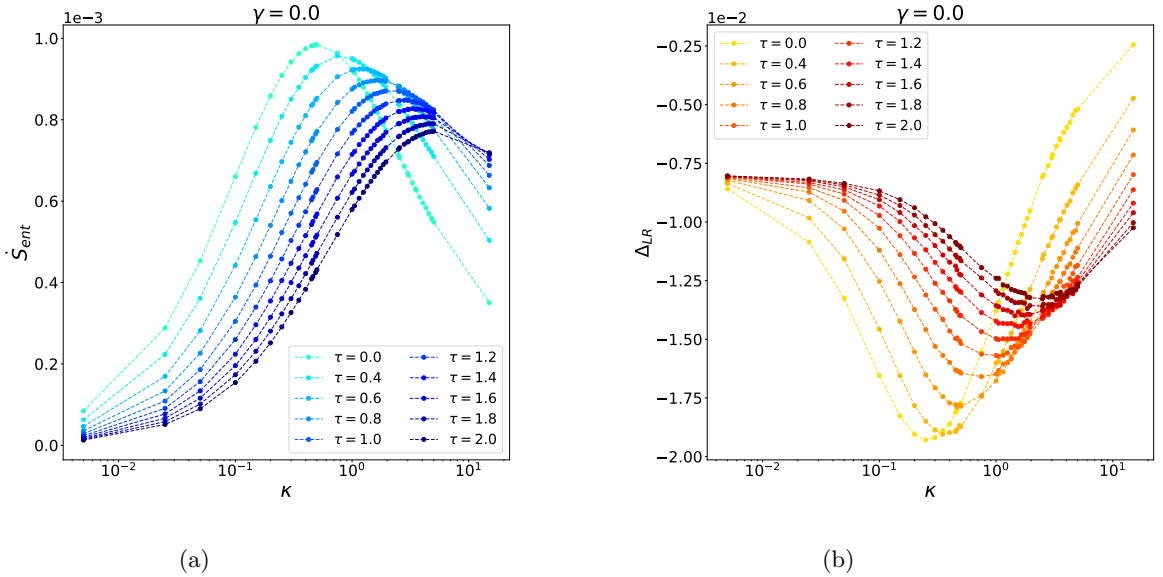


FIG. 2: Numerical simulation of stochastic Schrodinger equation (2) for $L = 160$ and $h = \sqrt{2}$. (a) Velocity of entanglement spreading \dot{S}_{ent} as a function of coupling to the stochastic field κ and (b) correlation function Δ_{LR} as a function of κ , in the long time limit. \dot{S}_{ent} and Δ_{LR} show a Zeno-crossover in the late time limit. For both quantities, we observe that the Zeno crossover occurs at larger values of κ , as the noise correlation time τ increases.

and \hat{N}_R is defined analogously. Eq. (23) serves as a proxy for transport properties across the dissipative site.

We use this quantity to probe the correlation formation in non-equilibrium steady state forming around the impurity (see Fig. 2b). Using the correlation matrix (22), we can evaluate (23) as follows

$$\Delta_{LR}^\eta = \sum_{i=-l}^{-1} \sum_{j=1}^l (-|C_{ij}^\eta(t)|^2 + |F_{ij}^\eta(t)|^2 + \delta_{ij} C_{ii}^\eta(t)). \quad (25)$$

V. RESULTS

Our numerical simulations reveal two key features of EE dynamics. First, we observe an expected linear growth of the EE [41] and second a non-monotonous behaviour of the EE's first derivative as a function of the coupling κ to the stochastic field (see Fig. 2a). The results presented for the $\gamma = 0$ case, qualitatively remain the same for $\gamma > 0$.

Both observations can be qualitatively explained with the quasi-particle picture for the entanglement entropy [41, 42], which has been also successfully applied in the XX chain subject to global noise [43]. In our case, the impurity emits highly entangled quasi-particle pairs travelling in opposite directions which entangle any two spatial sites at which the pair arrives simultaneously; this gives the the usual linear growth in time of the

entanglement entropy.

In the thermodynamic limit the light cone that originates at the driven site will take an infinite time to reach the edge of the system, hence the EE of the block we are studying will increase unboundedly. For the purposes of numerics, we terminate the simulations when $t \sim (2L + 1)/4$. The latter is the smallest time scale at which finite size effects start to appear.

The non-monotonous behaviour of the rate of change of EE can be explained by understanding the competition between the hopping strength and quasi-particle production from the impurity controlled by κ . Let us consider two limiting cases. In the Zeno regime, $\kappa \gg 1$, most of the quasi-particles produced remain trapped near the impurity site as the hopping term is too weak to transport them through the system. In the heating phase, $\kappa \ll 1$, the impurity produces a very small number of quasi-particle pairs (see, Fig. 3a) as compared to the Zeno-regime, and they spread across the system. When we increase κ in the heating side, we observe an increase in the number of quasi-particles which results in the increase of \dot{S}_{ent} (see, Fig. 3a). However, when $\kappa \sim 1$, we observe a Zeno crossover which can be seen as a transition from the regime where quasi-particles are delocalised throughout the system, to a regime where they are mostly trapped near the impurity site (see, Fig. 2a). As a consequence, inspite of having a very large number of quasi-particles as compared to the heating regime, we see a decline of \dot{S}_{ent} in the Zeno regime, because most of the quasi-particles will be unable to escape from a neigh-

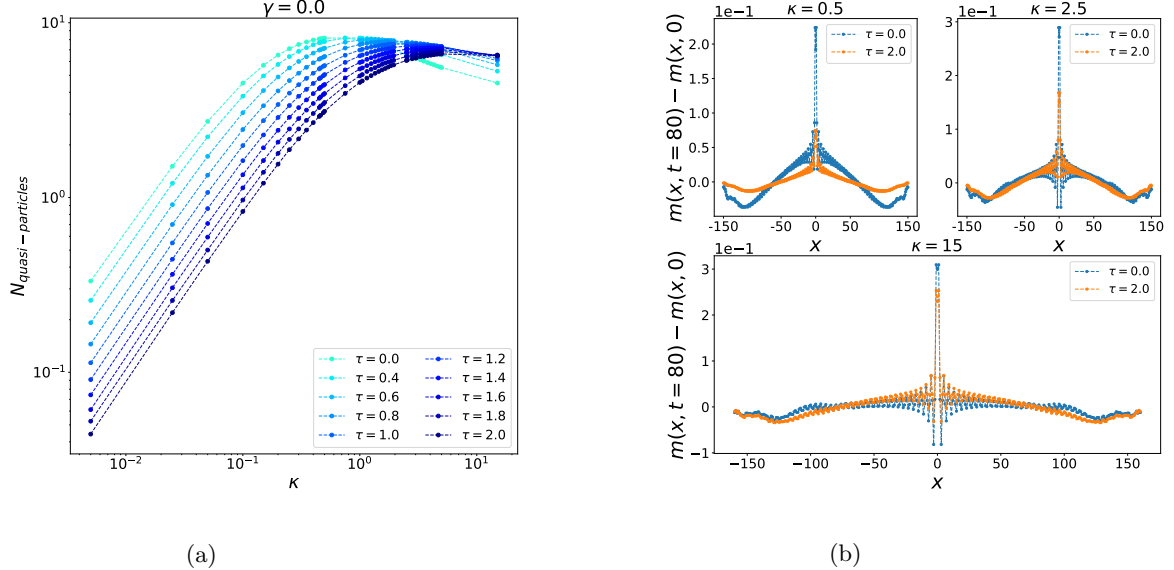


FIG. 3: Numerical simulation of the the stochastic Schrodinger equation (2) for $L = 160$ and $h = \sqrt{2}$. (a) Number of quasi-particles produced, N_{qp} , as a function of κ . We estimate N_{qp} on top of the initial magnetisation profile ($m(x, 0) \simeq 0.25$) at $t = 80$ ($N_{qp} = \sum_x |m(x, t) - m(x, 0)|$). In the heating regime, N_{qp} grows algebraically with κ . (b) Local magnetisation profile for $\tau = 0$ and $\tau = 2$. In the heating regime ($\kappa = 0.5$), most of the injected quasi-particle pairs result in the formation of a ballistic density front which starts from the impurity site and propagates towards the edge of the system, entangling $[0, L]$ with its complement. In the Zeno regime ($\kappa = 15$), we observe that, for $\tau = 2$, the trapping is attenuated with respect to $\tau = 0$. This reflects in the relative size of the ballistic density fronts observed in the two cases.

bourhood of the impurity.

A. Effect of a finite noise correlation time

In this subsection we discuss the effects of finite correlation time τ of the noise on the velocity of entanglement spreading in the heating and Zeno regimes. In the former the velocity of entanglement spreading reduces with an increase in τ (see Fig. 2a) as well as the total number of quasi-particle pairs injected by the impurity (see Fig. 3a).

In the Zeno regime $\kappa \gg 1$ we observe the exact opposite: the suppression of velocity of entanglement spreading reduces with increasing τ . This is attributed to the fact that as τ increases, the trapping of quasi-particles near the impurity site becomes less effective (cf. with Fig. 3b). This allows more quasi-particle pairs to participate in entangling the sub-system $[0, L]$ with its complement and hence we observe larger values of S_{ent} as τ increases. In other words, the tunnelling across the dissipative impurity becomes increasingly more coherent at larger τ and the Zeno effect is expected to attenuate; this explains a shift of the Zeno crossover to larger values of κ (cf. with Fig. 2a and 2b). We carried numerical simulations for larger values of τ and we could not find a critical value of τ where the Zeno effect completely disappears;

the only net effect of a dissipative impurity with finite correlation time is to extend the heating phase to larger κ .

Notice that there is a minor contribution to enhancement of S_{ent} in the Zeno regime from increased number of quasi-particle pairs for finite τ as compared to $\tau = 0$. However, the difference in number of quasi-particle pairs between $\tau > 0$ and $\tau = 0$ is much smaller than what is observed in the heating regime.

VI. PERSPECTIVES

The observation that the entanglement entropy can detect the crossover from the heating to the Zeno regime, opens to the perspective of connecting the field of dissipative impurities with a new class of non-equilibrium entanglement transitions recently studied in random hybrid circuits. In that context, the competition of unitary entangling gates with projective measurements result in a Zeno effect separating an area law and volume law phases, upon reducing the measurement rate [44]. Developing platforms where dissipative impurities can expose similar effects, could result in experimental proposals for detecting entanglement transitions using, for instance, cold atoms [45].

We believe that our results hold a certain level of gen-

erality. The local dissipative channel studied here contains, for finite anisotropy ($\gamma \neq 0$), both heating, pump and loss effects (cf. Eq. (15)), therefore, we expect that solving the problem with incoherent spin losses would lead to qualitatively similar results for the dynamics of the entanglement entropy. From a technical side, it could be interesting to apply methods for the exact solution of boundary driven problems [23–29] in order to extend our results to interacting versions of the free fermion model considered here. A relevant question is the possibility to morph the Zeno effect from a crossover into a sharp transition in the presence of interactions, and inspect the impact of a driving noise with finite correlation time on

such transition. Our current efforts are directed in this direction.

ACKNOWLEDGEMENTS

We thank B. Buca for constructive discussions. JM gratefully acknowledges P. Dolgirev, D. Sels and E. Demler for collaborations on related topics. A. C thanks R. Singh for helpful discussions and for the computational resources. The support and the resources provided by ‘PARAM Shivay Facility’ under the National Supercomputing Mission, Government of India at the Indian Institute of Technology, Varanasi are gratefully acknowledged.

-
- [1] I. Affleck, arXiv:0809.3474 [cond-mat] (2009), arXiv: 0809.3474.
- [2] G. D. Mahan, *Many-particle physics* (Springer Science & Business Media, 2013).
- [3] D. A. Zezyulin, V. V. Konotop, G. Barontini, and H. Ott, *Phys. Rev. Lett.* **109**, 020405 (2012).
- [4] G. Barontini, R. Labouvie, F. Stubenrauch, A. Vogler, V. Guarnera, and H. Ott, *Phys. Rev. Lett.* **110**, 035302 (2013).
- [5] B. Misra and E. G. Sudarshan, *J. Math. Phys.* **18**, 756 (1977).
- [6] W. M. Itano, D. J. Heinzen, J. Bollinger, and D. Wineland, *Phys. Rev. A* **41**, 2295 (1990).
- [7] P. Facchi and S. Pascazio, *Phys. Rev. Lett.* **89**, 080401 (2002).
- [8] A. Kofman and G. Kurizki, *Phys. Rev. A* **54**, R3750 (1996).
- [9] A. Kofman, G. Kurizki, and T. Opatrný, *Phys. Rev. A* **63**, 042108 (2001).
- [10] A. Kofman and G. Kurizki, *Nature* **405**, 546 (2000).
- [11] H. Fröml, A. Chiocchetta, C. Kollath, and S. Diehl, *Phys. Rev. Lett.* **122**, 040402 (2019).
- [12] M. Lebrat, S. Häusler, P. Fabritius, D. Husmann, L. Corman, and T. Esslinger, *Phys. Rev. Lett.* **123**, 193605 (2019).
- [13] L. Corman, P. Fabritius, S. Häusler, J. Mohan, L. H. Dogra, D. Husmann, M. Lebrat, and T. Esslinger, *Phys. Rev. A* **100**, 053605 (2019).
- [14] F. Tonielli, R. Fazio, S. Diehl, and J. Marino, *Phys. Rev. Lett.* **122**, 040604 (2019).
- [15] M. Schiro and O. Scarlatella, *The Journal of chemical physics* **151**, 044102 (2019).
- [16] F. Tonielli, N. Chakraborty, F. Grusdt, and J. Marino, *Physical Review Research* **2**, 032003 (2020).
- [17] C. Baals, A. G. Moreno, J. Jiang, J. Benary, and H. Ott, arXiv preprint arXiv:2012.11487 (2020).
- [18] A. Biella and M. Schiró, arXiv preprint arXiv:2011.11620 (2020).
- [19] A. Sartori, J. Marino, S. Stringari, and A. Recati, *New Journal of Physics* **17**, 093036 (2015).
- [20] T. Yoshimura, K. Bidzhiev, and H. Saleur, *Physical Review B* **102**, 125124 (2020).
- [21] A. Khedri, A. Štrkalj, and O. Zilberberg, arXiv preprint arXiv:2012.04628 (2020).
- [22] T. Maimbourg, D. M. Basko, M. Holzmann, and A. Rosso, arXiv preprint arXiv:2009.11784 (2020).
- [23] B. Žunkovič and T. Prosen, *J. Stat. Mech.: Theory Exp.* **2010**, P08016 (2010).
- [24] M. Žnidarič, *Phys. Rev. E* **83**, 011108 (2011).
- [25] T. Prosen, *J. Phys. A* **48**, 373001 (2015).
- [26] M. Žnidarič, *Phys. Rev. E* **92**, 042143 (2015).
- [27] W. Berdanier, J. Marino, and E. Altman, *Phys. Rev. Lett.* **123**, 230604 (2019).
- [28] B. Buča, C. Booker, M. Medenjak, and D. Jaksch, *New Journal of Physics* **22**, 123040 (2020).
- [29] V. Alba and F. Carollo, arXiv preprint arXiv:2103.05671 (2021).
- [30] H. Fröml, C. Mückel, C. Kollath, A. Chiocchetta, and S. Diehl, *Phys. Rev. B* **101**, 144301 (2020).
- [31] P. Krapivsky, K. Mallick, and D. Sels, *J. Stat. Mech.: Theory Exp.* **2019**, 113108 (2019).
- [32] T. Wasak, R. Schmidt, and F. Piazza, arXiv preprint arXiv:1912.06618 (2019).
- [33] S. Wolff, A. Sheikhan, S. Diehl, and C. Kollath, *Phys. Rev. B* **101**, 075139 (2020).
- [34] M. T. Mitchison, T. Fogarty, G. Guarneri, S. Campbell, T. Busch, and J. Goold, *Physical Review Letters* **125**, 080402 (2020).
- [35] P. E. Dolgirev, J. Marino, D. Sels, and E. Demler, *Phys. Rev. B* **102**, 100301 (2020).
- [36] S. Sachdev, *Handbook of Magnetism and Advanced Magnetic Materials* (2007).
- [37] C. Gardiner and P. Zoller, *Quantum noise: a handbook of Markovian and non-Markovian quantum stochastic methods with applications to quantum optics* (Springer Science & Business Media, 2004).
- [38] B. Bertini and M. Fagotti, *Journal of Statistical Mechanics: Theory and Experiment* **2015**, P07012 (2015).
- [39] M. Fagotti, *Journal of Statistical Mechanics: Theory and Experiment* **2014**, P03016 (2014).
- [40] L. Amico, R. Fazio, A. Osterloh, and V. Vedral, *Rev. Mod. Phys.* **80**, 517 (2008).
- [41] P. Calabrese and J. Cardy, *Journal of Statistical Mechanics: Theory and Experiment* **2016**, 064003 (2016).
- [42] P. Calabrese and J. Cardy, *Journal of Statistical Mechanics: Theory and Experiment* **2005**, P04010 (2005).
- [43] X. Cao, A. Tilloy, and A. De Luca, *SciPost Physics* **7** (2019), 10.21468/SciPostPhys.7.2.024.

- [44] Y. Li, X. Chen, and M. P. A. Fisher, *Phys. Rev. B* **98**, 205136 (2018).
- [45] R. Islam, R. Ma, P. M. Preiss, M. E. Tai, A. Lukin, M. Rispoli, and M. Greiner, *Nature* **528**, 77 (2015).